Future of medical physics: Real-time MRI-guided proton therapy

Bradley M. Oborn[a)]
Illawarra Cancer Care Centre (ICCC), Wollongong, NSW 2500, Australia
Centre for Medical Radiation Physics (CMRP), University of Wollongong, Wollongong, NSW 2500, Australia

Stephen Dowdell
Shoalhaven Cancer Care Centre, Nowra, NSW 2541, Australia

Peter E. Metcalfe
Centre for Medical Radiation Physics (CMRP), University of Wollongong, Wollongong, NSW 2500, Australia
Ingham Institute for Applied Medical Research, Liverpool, NSW 2170, Australia

Stuart Crozier
School of Information Technology and Electric Engineering, University of Queensland, QLD 4072, Australia

Radhe Mohan
Department of Radiation Oncology, MD Anderson, Houston, TX 77030, USA

Paul J. Keall
Sydney Medical School, University of Sydney, NSW 2006, Australia
Ingham Institute for Applied Medical Research, Liverpool, NSW 2170, Australia

(Received 11 December 2016; revised 12 March 2017; accepted for publication 15 May 2017; published 4 July 2017)

With the recent clinical implementation of real-time MRI-guided x-ray beam therapy (MRXT), attention is turning to the concept of combining real-time MRI guidance with proton beam therapy; MRI-guided proton beam therapy (MRPT). MRI guidance for proton beam therapy is expected to offer a compelling improvement to the current treatment workflow which is warranted arguably more than for x-ray beam therapy. This argument is born out of the fact that proton therapy toxicity outcomes are similar to that of the most advanced IMRT treatments, despite being a fundamentally superior particle for cancer treatment.

In this *Future of Medical Physics* article, we describe the various software and hardware aspects of potential MRPT systems and the corresponding treatment workflow. Significant software developments, particularly focused around adaptive MRI-based planning will be required. The magnetic interaction between the MRI and the proton beamline components will be a key area of focus. For example, the modeling and potential redesign of a magnetically compatible gantry to allow for beam delivery from multiple angles towards a patient located within the bore of an MRI scanner. Further to this, the accuracy of pencil beam scanning and beam monitoring in the presence of an MRI fringe field will require modeling, testing, and potential further development to ensure that the highly targeted radiotherapy is maintained.

Looking forward we envisage a clear and accelerated path for hardware development, leveraging from lessons learnt from MRXT development. Within few years, simple prototype systems will likely exist, and in a decade, we could envisage coupled systems with integrated gantries. Such milestones will be key in the development of a more efficient, more accurate, and more successful form of proton beam therapy for many common cancer sites. [https://doi.org/10.1002/mp.12371]

Key words: adaptive planning, magnetic deflection, magnetic field, MRI-guided proton therapy, proton beam

1. INTRODUCTION

1.A. Rationale for MRPT

A fundamental tenet in radiotherapy is that a decrease in dose will lead to a decrease in normal tissue toxicity. This principle has been examined and in many cancer sites supported as summarized through the QUANTEC reports.[1] Based on the physics and multiple planning studies of both passively scattered and actively scanned proton therapy, we would expect proton therapy to show markedly reduced clinical toxicity. However, this expectation is yet to be realized. A retrospective medical claims review of 27,000 IMRT patient and 550 proton therapy patients shows no statistically significant difference in toxicity.[2] Similarly, in a prospective randomized clinical trial (NCT00915005) of locally advanced nonsmall cell lung cancer, radiation pneumonitis was lower

in the IMRT arm than the proton therapy arm.[3] This mismatch between expected and observed outcomes leads to a compelling hypothesis: advanced image guidance is required to realize the clinical potential of proton therapy.

Given the longer history and larger number of systems, advanced image guidance in x-ray therapy is far ahead of proton therapy. A new and fast-growing area of x-ray-based therapy is integrated MRI-x-ray systems. MRI offers the potential for both real-time anatomic imaging and also physiologic imaging with the patient in the treatment position. Merging MRI with proton therapy provides a compelling opportunity to realize the clinical potential of proton therapy and also explore further improvements in patient care through monitoring and adapting to changing tumor and normal tissue physiology throughout a course of radiotherapy.

As a final note, we consider the recent Point/Counterpoint article by Paganetti and Yu[4] entitled "*Photon radiotherapy has reached its limit in terms of catching up dosimetrically with proton therapy*". In this discussion, the "ceiling" for proton therapy quality is described as being higher than for photons, despite not being reached yet in either discipline. A development that would significantly raise both the quality and the ceiling of proton therapy is that of the implementation of real-time MRI guidance.

1.B. Current state of the art in MRXT

Real-time magnetic resonance or MR-guided x-ray beam radiotherapy, MRXT, was launched clinically in 2014 with the introduction of the ViewRay MRIdian system, consisting of a 0.35 T MRI scanner coupled with a three-head Cobalt-60 radiation source.[5] At present six sites around the world are operating with the MRIdian system,[6] with at least two more confirmed for operation in early 2017.[7] Development and progress of this system is detailed in no less than 18 articles.[8] We also note the development of the linac-based MRIdian system for nonclinical research.[9] Production of other preclinical linac-based MRXT systems is also well underway with the development of the Philips-Elekta system Unity.[10] This consists of a Philips 1.5 T MRI scanner coupled with an Elekta 7 MV linear accelerator. Currently, these systems are still being installed and tested under a research consortium arrangement in seven sites around the world.[11] Clinical treatments are planned before the end of 2017, and at least 37 publications are listed related to the development of the world's first high-field MRI-guided x-ray therapy system. Another commercial linac-based program by MagnetTx[12] is developing the Aurora RT system, consisting of a 6 MV x-ray beam and a rotating bi-planar 0.5 T magnet with an iron yoke.[13] This program describes 44 publications around the development of the world's first inline orientation MRI-linac system.[14] Finally, there is a 1 T split-bore magnet research system under development at the Ingham Institute in Sydney Australia.[15,16] This system is the world's first high-field strength inline system with an air-core MRI. At present, at least 30 publications are related to this program.[17]

1.C. Existing literature in MRPT

Considering the potential improvements of MRPT over conventional proton therapy as outlined in the Section 1.A, various groups have performed simulation-based studies of the feasibility of some aspects of MRPT. Several studies have looked at the fundamental beam transport and dosimetry changes, in particular, the magnitude of the deflection of proton beams by the strong magnetic fields typically found in the imaging volume of an MRI scanner. These include estimation of the deflection inside a water phantom by Raaymakers et al.[18] and Wolf and Bortfeld.[19] Optimized patient-based planning in uniform magnetic fields to account for the imaging field deflection has also been studied by Moteabbed et al.[20] and Hartman et al.[21] These studies assumed a static external magnetic field without fringe field effects as being the influence of the MRI scanner. It has been shown recently, however, that the fringe field of an MRI scanner has a complex and significant impact on how a proton beam transports towards the MRI isocenter.[22] A important implication of this work is that the most reliable method for proton beam delivery in real-time MR-guided proton therapy will be the pencil beam scanning method. Passively scattered broad beams, which also contain a broad energy range, will deflect and distort as they travel through the 3D spatially variant fringe field and deposit their Bragg peaks at locations different from the nonmagnetic field case. On the contrary, the pencil beam scanning method will require simple spatial correction on a per-pencil-beam basis in order to achieve the correct Bragg peak locations for each pencil beam.

In the area of MRI-only-based planning for protons, several papers have been published. In 2013, Rank et al. reported on the use of a classification-based tissue segmentation method based on discriminant analysis to derive so-called pseudo CT numbers from MR images of three patients with lesions in the brain.[23] The main issues encountered were challenges with assignment of air and bone regions. Dosimetrically, the proton beam plans only had small or clinically acceptable deviations from reference CT-based comparison plans. Also in 2013, Rank et al. reported on a more generic conversion study of MR images for proton beam planning.[24] MRI datasets were acquired for three different samples of pork chops using up to eight different contrast agents. Again, issues arose related to bone definition which led to some more significant dosimetry differences with respect to CT-based reference dataset plans when using proton beams. In 2014, Edmund et al. investigated five MRI-based brain tumor cases with proton beam plans.[25] Pseudo CT datasets were generated by three methods including threshold-based segmentation, Bayesian segmentation, and statistical regression. Dose agreement to within 2% was observed with reference CT-based plans for the most promising statistical regression method. An important finding reported was that the number of tissue grades defined impacted the dosimetry match with the reference CT dose plans. In more recent work by Koivula et al.,[26] the feasibility of using MRI for both brain and prostate cancers has also been studied. In this work substitute CT

datasets were generated by transforming the intensity values of in-phase MR images to Hounsfield units with a dual model HU conversion technique to enable heterogeneous tissue representation. Proton plans using the substitute CT dataset matched to the reference CT-based plans with a 91% gamma pass rate at 1%/1 mm tolerance. Overall the authors conclude that an MRI-only planning workflow is feasible for proton therapy of the investigated brain and prostate plans.

As a final comment on the current MRPT-related literature, we note the 2011 review paper by Schippers and Lomax.[27] In this article entitled "*Emerging Technologies in Proton Therapy*", a small section was dedicated to the concept of the integration of MRI with proton therapy. The most challenging aspects were listed as compensation of the influence of the MRI field on the proton beamline transport magnets, as well as the magnetic field effects on beam monitoring systems.

In summary, the current literature supports the feasibility of MRI-guided proton beam therapy from a fundamental patient dosimetry viewpoint. Good progress has been made for MR-only planning of relatively static tumor sites but there is a clear need for further development of the more dynamic tumor sites. There are however no studies dedicated to the larger scale questions such as the operation of a proton beam delivery system in the presence of an MRI scanner, or the design requirements for this unique piece of as yet unreleased advanced radiotherapy equipment. In this *Future of Medical Physics* paper, we describe the key software and hardware considerations for development and implementation of real-time MRI-guided proton beam therapy. Figure 1 provides a summary of these key aspects. The various elements in Fig. 1 are discussed in detail throughout the remainder of this article. Section 2 provides a general overview of the potential workflow in MRPT. Section 3 summarizes the software considerations starting from MR-based dose planning to real-time adaptive planning. Section 4 discusses the important hardware considerations, while Section 5 details various prototype concept designs. Finally in Section 6, our vision for working towards MRPT is detailed, with predictions regarding the pathway forward in various key research areas.

2. WORKFLOW IN MRXT AND MRPT

2.A. MRXT workflow

There are various proposals and methods for the workflow of treating patients in MRXT. One such workflow which is possible on the ViewRay MRIdian system is gated treatments with online adaptive replanning before each fraction to account for patient anatomy changes since the last fraction.[28] During this type of approach, the patient undergoes an MRI scan at the start of each fraction and that information is registered back to the original planning image dataset. This original planning dataset may be CT- or MRI-based, depending on the desired workflow. From there, an updated or adaptive plan is then produced, and subsequently is delivered calculation before beam with MRI-based gating. In this gating technique, the beam is delivered only when there is sufficient alignment with the real-time observed GTV (or greater organ containing the GTV) and the original planning stage GTV. At present, this alignment is based on the real-time sagittal cine MR images. A history of the patient anatomy during beam on is also recorded via the MR images obtained, as well as a log of the machine and/or radiation beam parameters. This information is then also available for consideration in producing the adaptive plan of the next fraction. This process of plan adaptation at the start of each fraction continues until all fractions are delivered. The gated adaptive approach is reasonably transparent and so offers confidence in delivering radiation during real-time MR guidance. The primary downside to this method is the increased treatment times through at least three processes: (a) preirradiation imaging acquisition, (b) adaptive replanning calculation before beam delivery, and (c) gating of beam delivery, particularly for highly dynamic tumors. The second point can be addressed through fast dose planning calculation methods. One method to avoid the third effect would include dynamic MLC tracking movements throughout the entire patient breathing cycle. In this approach, there is greater postprocessing required to combine and register all patient doses and anatomy back to the original static plan. There may also be some effects with latency of MLC leaf motion not providing the ideal beam shape with time; however, preliminary clinical data from non-MRI-linac systems are showing great promise.[29]

With regard to patient-specific quality assurance (QA), we note the process followed for the real-time adaptive plan QA performed on ViewRay system while the patient is on the treatment couch.[30] In this process, all the updated plan details are exported through an independent format, i.e., DICOM, to an in-house dose plan check system based on Monte Carlo methods. This system recalculates the new adaptive plan doses independently and provides a gamma calculation pass-rate as compared to the original TPS dose prediction. Further to this, setup verification localization images are acquired at the start of each fraction, and machine log file analysis is performed after all fractions.

2.B. MRPT workflow

At first consideration, an online adaptive replanning workflow with static or breath-hold gated treatments would be a natural implementation for MRPT. An initial CT scan would be used for planning and all future MRI datasets (daily preirradiation and intrafractional if acquired) would be registered back to this original CT dataset and plan. It would be expected that all treatments be delivered by the pencil beam scanning method for the reasons outlined in Section 1.C. In highly static tumor treatments such as brain cancers, the process of imaging, adaptive replan, and static treatment will be relatively straight forward. The improvements offered via the onboard MR images will be clear over conventional offline CT/MRI methods. Firstly, the patient will be imaged in the treatment position. Secondly, any daily anatomy changes and/or tumor margin changes will be known and refined with the highest possible accuracy. For each fraction, a pencil beam

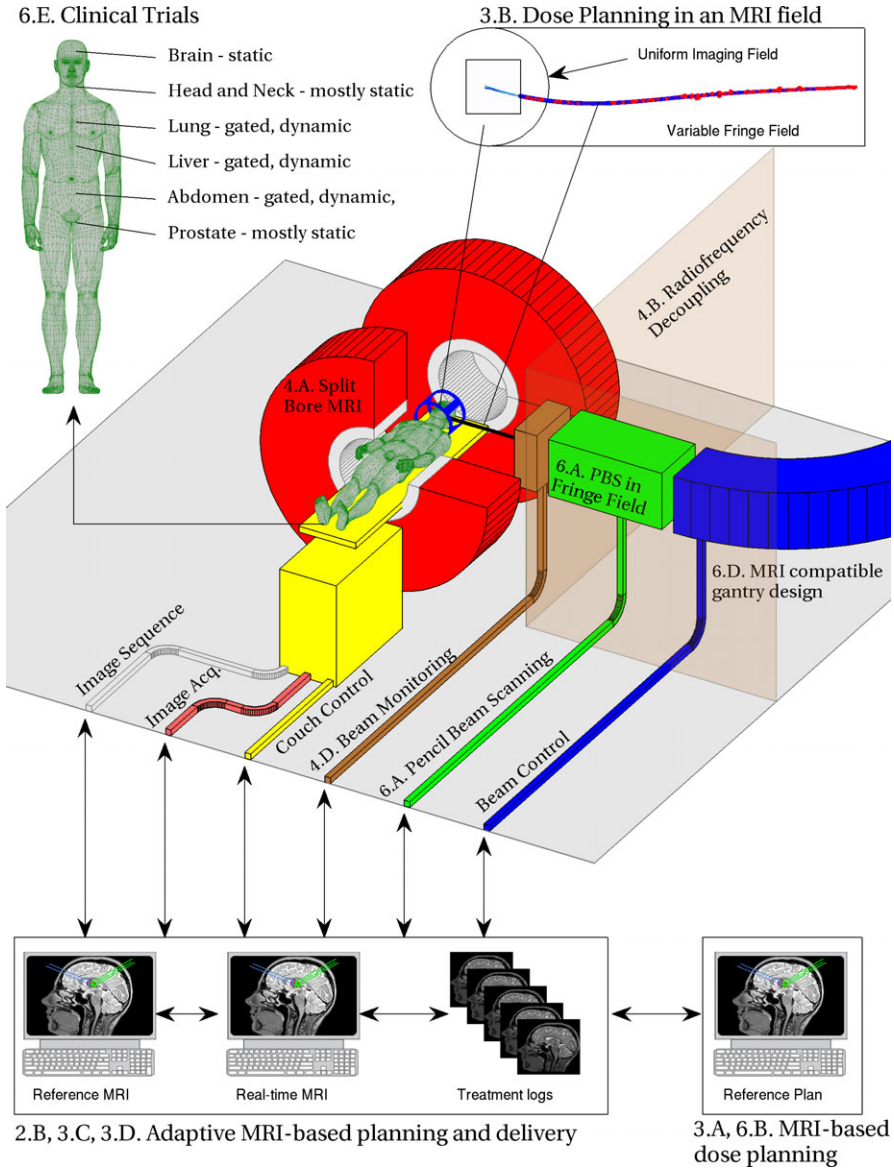

FIG. 1. Schematic diagram of the software and hardware aspects envisaged in the development of MRI-guided proton therapy (MRPT). The key areas of development for an MRI-only workflow will be MRI-based planning, proton beam delivery and monitoring in magnetic fringe fields, and adaptive treatment methods. [Color figure can be viewed at wileyonlinelibrary.com]

scanning treatment will then cover a tumors' accurately defined 3D target volume with zero-dose image guidance.

In principle, the former process should also be the case for dynamic or moving tumors which are treated with breath-hold gating. The 3D outline of a tumor will be known with highest accuracy, over a small timeframe, where fast scanning pencil beams build-up dose to cover the entire treatment volume. The only difference in this case should be longer treatment times to account for the beam-hold durations.

In the most advanced case of free-breathing treatment, there may be some tumor motion while the beam is being delivered, depending on cancer type. With pencil beam scanning treatments comes the potential for interplay effects.[31,32,33] These effects, i.e., possible significant hot or cold spots within the treatment volume accumulated over the course of a single fraction, are shown to be mitigated by fractionation,[32] multiple rescanning,[33] and retracking.[34] In the case of MRPT, the real-time MR images at the rate of 4–8 frames per second may in fact be available to assist in the management of interplay effects. It may be possible to track in real-time a tumor margin and correspondingly alter or translate the pencil beam scanning pattern. The exact method will likely take a path that is governed by the advances in its accuracy, reproducibility, and proven effectiveness.

With regard to patient-specific QA, one would expect a workflow similar to that outlined in Section 2.A for MRXT. In the case of proton beam planning however, small anatomy changes may introduce large changes to the pencil beam scanning pattern for each beam. We expect that an extra step will be required to determine the robustness of any new adaptive plan. Ideally this would be completed quickly at the end of the independent dose calculation.

In conclusion, the workflow in MRPT would likely naturally take a direction similar to that currently unfolding in MRXT. The first stages being daily adaptive replanning for static tumors that have moved or changed over the patients' treatment course. The next stages would likely be adaptive replanning with breath-hold gating to ensure that a static anatomy is treated. As the modality advances, users would be naturally eager to assess the usefulness of the real-time MR guidance for dynamic tumors.

3. SOFTWARE CONSIDERATIONS

3.A. MRI-only proton therapy planning

In Section 2.B, the workflow described for MRPT assumed the reference plan to be calculated using patient CT images. This approach will be the most robust in the early stages of MRPT, as CT-based planning is considered the best practice for estimation of patient composition for dose planning. In fact recent publications are showing promise for proton beam range calculation uncertainties to be in the order of 1% error with the use of dual energy CT (DECT).[35,36,37] A potential initial workflow in MRPT would then be to register daily MR images back to the original planning CT dataset. This would accurately account for any patient anatomy changes, provided that there is confidence in the deformable image registration process for the given anatomical site. In this process, the superior soft tissue delineation offered by the MRI data would be registered onto the CT planning dataset. However with MRXT, there has been success in directly converting MRI to pseudo or substitute CT images which can accurately reproduce the electron density information used for dose planning.[38,39,40] Such methods eliminate the requirement to acquire an initial patient CT dataset, while preserving the inherent soft tissue delineation shown in the MRI data. As described in Section 1.C, similar studies have been performed for proton therapy-based planning with mixed but promising results. It would appear a natural quest for the pathway of MRPT to be MRI-only planning-based; however, the process needs to be completely robust and superior to the current CT-based planning process. We expect that many novel approaches will need to be considered, developed, and tested in the path to finding methods for performing accurate proton beam dose calculations on MRI datasets.

3.B. Dose planning in magnetic fields

In MRXT, the primary therapeutic x-ray beam propagates towards and through the patient and the treatment volume without being perturbed by the MRI scanner field. Dose planning in MRXT can then be modeled (almost entirely) by calculating the magnetic field induced effects on the dose depositing secondary electrons liberated by the primary x-ray beam. The MR imaging volume, by its nature, is highly uniform in direction and magnitude and encompasses the patient volume around the isocenter of the MRI scanner. Hence, the process of dose planning in MRXT is mostly dependent on the nominal strength and direction of the MR imaging field. We do note however various effects on the transport of any air-generated secondary electrons produced by the parent x-ray beam. These may be above the patient, or scattered from the patient on the exit side.[41,42,43,44,45,46,47,48,49,50]

With MRPT, the therapeutic proton beam (being charged particles), is subject to the Lorentz deflection force when transporting towards the patient at the center of the MRI, as well as within the patient while slowing down. The planning process is best broken down into two components as described in Fig. 1: (a) pencil beam scanning and transport towards the planning volume (transport through a fringe field), and (b) pencil beam transport within the planning volume (patient and immediate surrounding volume at fixed magnetic field and direction). These are described further below:

a. Fringe field transport: pencil beam scanning and fringe field deflection. This will be specific to MRPT design, namely the beamline design and integration method between the MRI and scanning magnets. A full accurate model and experimental evaluation of this coupled process will be required to accurately determine the properties of the pencil beams as they enter the planning volume. Without a magnetic field, all pencil beams entering the planning volume arrive at this boundary with a direction vector that is simply related to how far off-axis the pencil beam is, or how much it was scanned. In the case of MRPT, this will not be true. There will be complex deflections within the fringe field that changes the direction vectors. This is also energy and spatially dependent. Thus, this process needs to be 'mapped out' for all cases, i.e., field sizes and beam energies. A look-up-table (LUT) of these data for each unique MRPT design should then be built and used as input to the next stage of dose planning as outlined in the next section.

b. Patient dose calculation. The patient will be encompassed, for all intensive purposes, by a uniform magnetic field value equal to the MRI strength and direction. Thus, dose calculations are straight forward with optimizing pencil beamlets, read in from the LUT, that then account for the uniform field inside the 'planning volume'. The latter component of this approach has been performed already in previous works where the extent of the uniform imaging field is 70 cm in diameter.[21]

The true advantage of separating the dose planning into the two components mentioned above is that, once part (a) is completed for a unique MRPT design, then the LUT of data describing the fringe field deflection and pencil beam scanning process can be passed onto independent dose planning engines. The only requirement is that plans must be optimized according to the planning volume boundary specified in the LUT. It would therefore be a natural quality assurance process to regularly confirm the accuracy of the LUT data against measurements. The integration of the MRI and proton beamline would need to be monitored routinely after commissioning.

3.B.1. Pencil beam scanning and fringe field correction: an example

In the previous section, the beam modeling through an MRI fringe field was described. We provide here an example of this process for the magnetic field of the Agilent 1 T split-bore design for the Sydney MRXT prototype.[22]

Figure 2 demonstrates this concept for a simple case in the perpendicular orientation (see Section 4.A) using simple Monte Carlo simulations. In Fig. 2(a) a 170 MeV pencil beam travels into a 30 cm^3 water phantom with direction along the x-axis without any external magnetic fields. The Bragg peak occurs at around 190 mm depth, and is located, as expected, on the central axis. The pencil beam started at 2 m from the isocenter, around the same location as they would exit the PBS assembly in the IBA Universal Head. This emulates a nonscanned 170 MeV proton pencil beam as it exit the PBS assembly.

In Fig. 2(b), we present the required beam to match the Bragg peak location obtained with Fig. 2(a) when the 1 T split-bore MRI field is present. In this case, there is mostly transverse fringe field, giving rise to a perpendicular deflection in the +z direction. Thus, one needs to apply a scan setting in the −z direction to reverse this effect. In our modeling example, this is emulated via a small initial momentum vector component in the −z direction as detailed. The next element to consider is that the path taken to reach the same Bragg peak location is now longer than the nonmagnetic field case. Hence, an increase in energy is also required. Using an iterative, forward Monte Carlo trial and error process, we have deduced that to align Bragg peaks, an increase of 3 MeV is required, coupled with a small initial −z

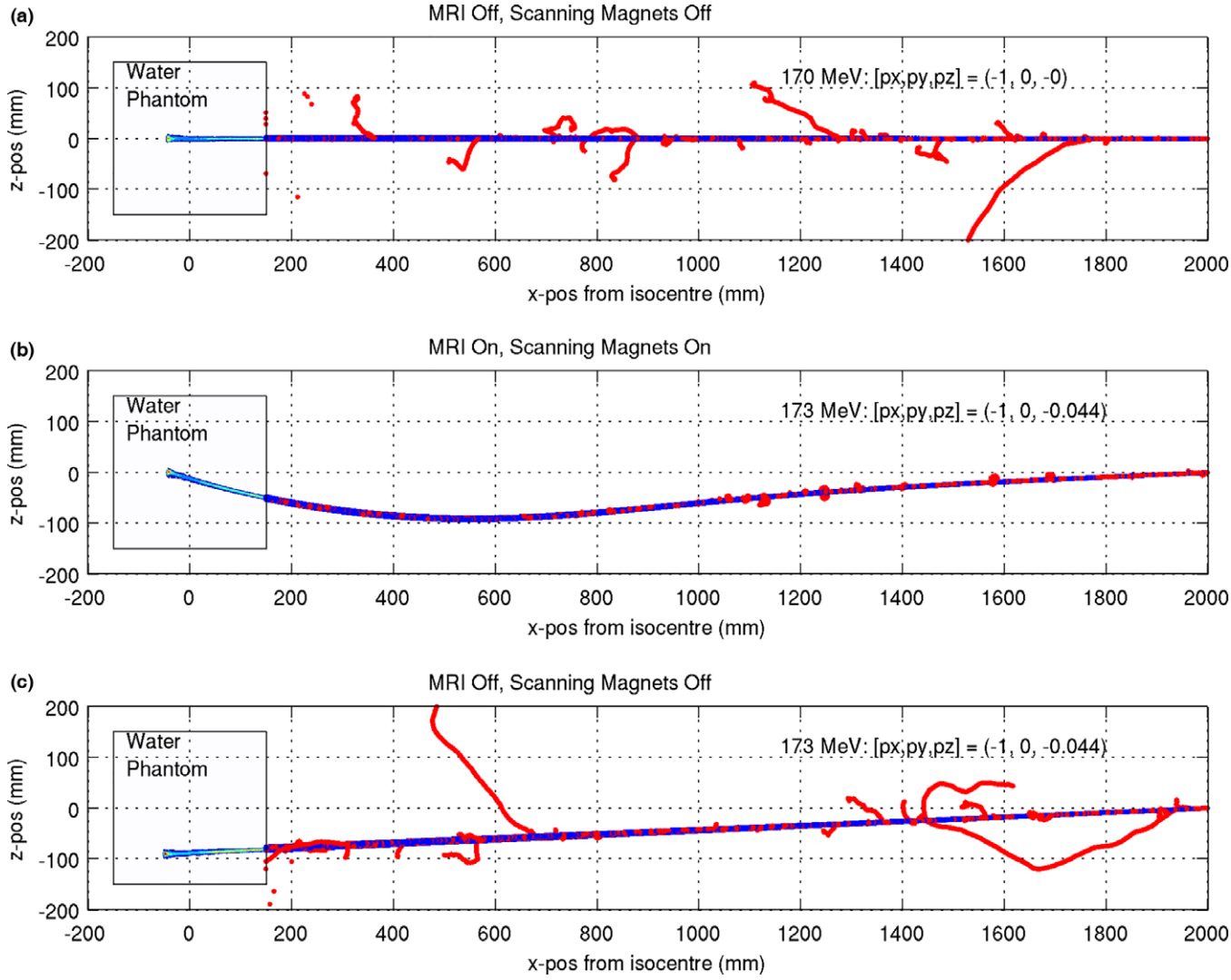

FIG. 2. Example of the correction to the pencil beam scanning process in the perpendicular orientation. In (a) a 170 MeV pencil beam (without a magnetic field) is incident along the x-axis (direction vector = [−1 0 0]). The Bragg peaks occurs at around 190 mm depth in a water phantom. In (b) a 173 MeV pencil beam is fired in the presence of the MRI field (perpendicular orientation) with a direction vector of [−1 0 −0.044]. The Bragg peak occurs at the same location, 190 mm depth. Without the MRI field, the 173 MeV proton beam would have its Bragg peak at 197 mm depth, and 90 mm off axis, as shown in (c). [Color figure can be viewed at wileyonlinelibrary.com]

momentum component. In Fig. 2(c), we see exactly how much the −z momentum shift would relate to without a magnetic field; about 90 mm deflection at the isocenter plane. Using this simple example, it can be seen that each and every pencil beam (energy and spatial location) will need unique corrections to account for the MRI fields. In the first case, a solution to this issue unique to MRPT is expected to be an experimental process during commissioning stages. An appropriate detector system will be required to determine the actual pencil beam location as it crosses the detector plane and software would link this to the scanning magnet settings and beamline energy. From there software-based static correction maps would be used for beam delivery.

3.C. Real-time adaptive planning with gated treatments

The adaptive treatment technique described in Section 2.A is a natural choice for delivering MRPT. The software requirements for this approach include fast online adaptive planning. The process of acquiring the prefraction MRI and then creating an adaptive plan needs to be performed as quickly as possible while the patient is waiting on the treatment couch. At present dose planning for pencil proton beam therapy is performed using both numerical and pseudo Monte Carlo-based methods. The inclusion of the magnetic fields in the planning volume now needs to be considered in these planning stages. Various fast graphical processing unit (GPU) Monte Carlo-based calculation methods have recently been reported for proton beam therapy planning.[51,52] Such systems may be ideally suited for fast online adaptive replanning; however, data transfer rates are further considerations that may limit the speed as compared to conventional CPU parallelization.

3.D. Real-time adaptive planning with dynamic treatments

The more advanced treatment case for MRPT is that of dynamic treatments, i.e., a moving PTV is targeted dynamically by the proton pencil beams rather than using gating. This approach will require seamless integration between the MRI system, planning system, and beamline control system. During treatment, the MR images would be processed in real-time to highlight and track the PTV. From there the real-time shifts in the pencil beam will be applied so that the delivered dose follows the moving target. It is notably more complicated than MRXT as the beams are pencil beams with a defined range (i.e., not broad beams which pass right through the PTV) and so there is some time taken to "paint" dose to a moving 3D volume. We can expect that the fundamental limit to the flexibility of this beam delivery method will be the time required to change the proton beam energy, i.e., Bragg peak depth. This is because the scanning process is controlled rapidly by adjusting scanning bending magnet currents, while changing the beam energy typically involves movement of physical graphite attenuators in and out of the beam path.

In any case, there may be the potential to optimize the beam delivery angle to be perpendicular to the tumor motion such that the proton beam energy or range needs minimal adjustment to account for the motion. This optimization however does depend on any other changes in the patient anatomy along the beam path which would require an energy change. Overall, using an optimized beam delivery angle will take advantage of the fast lateral scanning magnet deflection process over the slower energy change process. We do note however the study by Chaudri et al. which details the feasibility of using fast magnetic deflection (and recovery) of the pencil beam across a static degrader wedge to change the energy.[53] Such a method could significantly reduce the energy changing times over conventional moving wedge methods.

Similarly to gated treatments, it would be expected that all the delivered beam and patient anatomy information would be recorded and would form inputs to the adaptive replanning performed at the start of each fraction.

3.E. Biologically based adaptive planning: potential for subvolume boosting

From the outset of this section, we note that the radiobiology of proton beams is complex and debated in the literature. An excellent review paper has been published by Paganetti[54] which details several of these complexities. In the context of the current article, it is fitting that we describe a vision for how biological information, realized through the inherent daily MR images could be used to optimize a patient treatment.

In the default case, the daily fraction MR images acquired for adaptive planning purposes will be obtained with imaging sequences that are designed for anatomical accuracy. It may be possible in MRPT to also acquire image datasets with alternate sequences that highlight some element of the underlying biology of the tumors response to the radiotherapy. As an example, we shall consider the ability of MRI to determine tumor hypoxia. An excellent review and corresponding article have been recently published which details the ability of oxygen-enhanced MRI methods to predict tumor hypoxia in mouse subjects.[55,56] These articles detail compelling arguments for the successful translation of this technology to human subjects. If successful, the daily setup MR images could be complimented with these functional images. This information obtained could ultimately guide any decisions to boost dose to say some biological hot spot or subvolume within the gross tumor volume. With regard to proton therapy, it may be possible to boost dose to specific subvolumes of the tumor with relative ease, as compared to x-ray therapy. This is due to the inherent ease of manipulating the Bragg peak within a planning volume without compromising the remainder of the treatment plan, or alternately delivering more dose to specific tumor subvolumes in the pencil beam scanning plan. In the case of x-ray beams, boosting to a small subvolume would often require multiple beam angles and hence be a more complex change to the default radiotherapy plan.

4. HARDWARE CONSIDERATIONS

4.A. Magnet design requirements

An ideal magnet design to enable MRPT would be that of a split-bore MRI, such as the General Electric Signa-SP where two magnet poles are physically separated by an air gap. This would allow an unobstructed path for the proton pencil beam to reach the patient, and then allow this to be incident from many angles perpendicular to the patient head–feet axis. With a split-bore design however, there are two approaches in how to position a patient with respect to the magnet axis. In the simplest case, the patient lies along the bore of the MRI, identical to current MRI scanning. Thus, the magnetic field of the MRI scanner (inside the imaging volume) is perpendicular to the radiation beam. This is known as the perpendicular (or transverse) orientation. In this orientation, the radiation beam can be incident from many angles by employing a rotating gantry, or alternately via axial rotation of the patient along the head–feet axis using an axially rotating couch system. The alternate case, the inline orientation, is where the patient lies between the two halves of a split-bore magnet. The magnetic field inside the imaging volume is therefore inline (or parallel) with the radiation beam direction, which is directed down the magnet bore. With this orientation again you have two options on how to deliver a radiation beam from multiple angles. The simplest case is to axially rotate the patient along the head–feet axis via a rotating couch. The second approach is to rotate the entire MRI and radiation source around the patient. We note that the Sydney inline MRXT prototype envisages an axially rotating couch while the Aurora RT inline MRXT design uses a rotating magnet.

4.B. Radiofrequency (RF) shielding requirements

MRI scanners are typically housed inside RF shielded rooms to eliminate the influence of external RF signals perturbing the signal received from the patient during imaging. RF shielding (or Faraday cages) typically takes the form of a complete closed layer of around 1 mm of copper sheeting on the MRI room walls, floor, and roof. A typical exception to this is a Faraday filter (or waveguide port) through this layer to allow for cabling (power supplies, cooling, or similar) to pass into the MRI room without letting in external RF. These waveguides are essentially copper tubing with a length that is around 5 times the diameter of the tube. Such an arrangement attenuates any RF signals that try to pass through, however acts as a physical hole to allow for the cabling to pass through.

For MRPT, it is wise to assume that the components of the proton pencil beam scanning system and gantry will be a potential source of RF that must be shielded from the MRI. The majority of this can be RF shielded by enclosing the beamline with a copper shielding layer. The pencil beam would however need to pass through a thin layer of copper (or at least an RF conducting material) which will affect the pencil beam properties. The obvious solution here (to eliminate the beam passing through a copper or RF layer) is to deliver the pencil beam through an RF filter or long copper tube with length at least 5 times the diameter as described earlier. This is well suited to be positioned in the gap between the MRI cryostat halves or down the MRI bore.

4.C. Axial patient couch rotation vs gantry rotation

In the Sydney MRXT prototype, the patient would rotate along their head–feet axis during treatment via an axially rotating couch. This eliminates the need to rotate the x-ray source around the patient, and in so, greatly simplifies the beam delivery process. This does however come at the cost of increased plan complexity from the corresponding deformation due to patient rotation. In conventional CT-based radiotherapy planning, this process would be far from ideal. Separate patient CT scans at each beam angle where radiation would be planned and delivered may be required, resulting in increased imaging dose and multiple plans that would need coregistration. However in the case of MRXT/MRPT, the planning images are zero-dose, and the planning/treatment process is expected to be real-time and adaptive beyond the first fraction. Therefore no issues with excess imaging dose will be present, and planning datasets would be available for all patient anatomies treated. Another issue is potential patient discomfort with the rotation during treatment. A limited angle of couch rotation may reduce this discomfort. The advantage of MRPT with a rotating patient would be a major reduction in the cost of the unit. Without the need for a gantry, one only needs a static beamline, such as in a "fixed-beam" treatment room. An important point to note here is the recent work by Yan et al. where the necessity of the proton gantry was studied, based on 10 yr of clinical proton therapy treatments at MGH in Boston[57]. In this work, the most important finding was that >99% of patients treated with PBS could be treated with a fixed beam arrangement. In Sections 5.A.1 and 5.B.1, we detail MRPT prototype designs with gantry-less or fixed beamlines. Such designs would clearly be less complicated and less expensive. The driving force therefore behind gantry enabled designs (Sections 5.A.2 and 5.B.2) would be the ability to provide an essentially unrestricted beam entry angle around the patient, or more precisely, the best possible healthy tissue sparing with maximum patient comfort.

4.D. Beam monitoring systems

Current methods for PBS monitoring typically involve the use of multiwire ion chamber arrays to determine the location of the pencil beam at any time during scanning. In the case of MRPT, the ion chamber arrays may be located in strong MRI fringe fields. For example, the IBA Universal Head has the ion chamber located at approximately 850 mm from the isocenter. In the Sydney 1 T split-bore MRI design, this equates to a fringe field of

around 0.25 T. The overall impact that this will have on their operation is essentially unknown at this point in time. With regard to fundamental energy deposition processes, in air a proton pencil beam gives rise to secondary electrons which are ultimately the particles collected by the ion chamber wires. These are generated through either multiple Coulomb scattering within the thin windows of the ion chamber covers or with air molecules surrounding the wires. In the default case (B = 0 T), these secondary electrons travel away from the pencil beam in a symmetrical forwardly directed nature and so the ion chamber collects an accurate representation of each pencil beam. In the presence of a fringe field, there may be dramatic changes to this process as the secondary electrons are easily moved by the strong magnetic fields. This area of MRPT development will require investigation. Modeling may provide some early insight into the expected performance of multiwire arrays however experimental testing will ultimately be required to confirm the accuracy of such devices in magnetic fields.

4.E. Pencil beam scanning correction

Based on the discussion in Section 3.B.1, it can be foreseen that the vast majority of the pencil beam scanning correction process to be software-based. In particular, calibrations will be performed which map out the fringe deflections for a particular MRPT system, and direct corrections applied to the scanning magnet currents for each desired spot. However if this is not feasible, for example, the scanning magnets are not strong enough to recover the natural deflections encountered, then a solution would be to globally offset or twist the entire PBS assembly and beamline to account for these deflections seen. We note that this may only be an issue for an MRPT system that is perpendicular in orientation, as this sets up a transverse deflection. For an inline system, the deflection is a rotation about the beam central axis.[22]

5. POTENTIAL MRPT SYSTEMS

Throughout this section, we will demonstrate the concept of MRI-guided proton therapy using a model of the 1 T split-bore MRI used in the Sydney MRPT prototype. This is chosen as we have an accurate knowledge of the fringe field for this specific design.[44] Different magnet-to-proton beamline designs are also possible, with different field strengths respectively. To give credibility to the concept of MRPT, the key elements (i.e., the PBS assembly) of the IBA Universal head are shown in the position that they would be naturally with respect to a patient. We also introduce elements that would be unique to MRPT — an RF shielding layer to decouple the MRI from beamline, and novel dosimetry systems for PBS inside fringe magnetic fields. Finally, the two beam-to-magnetic field orientations familiar with MRXT are presented (perpendicular

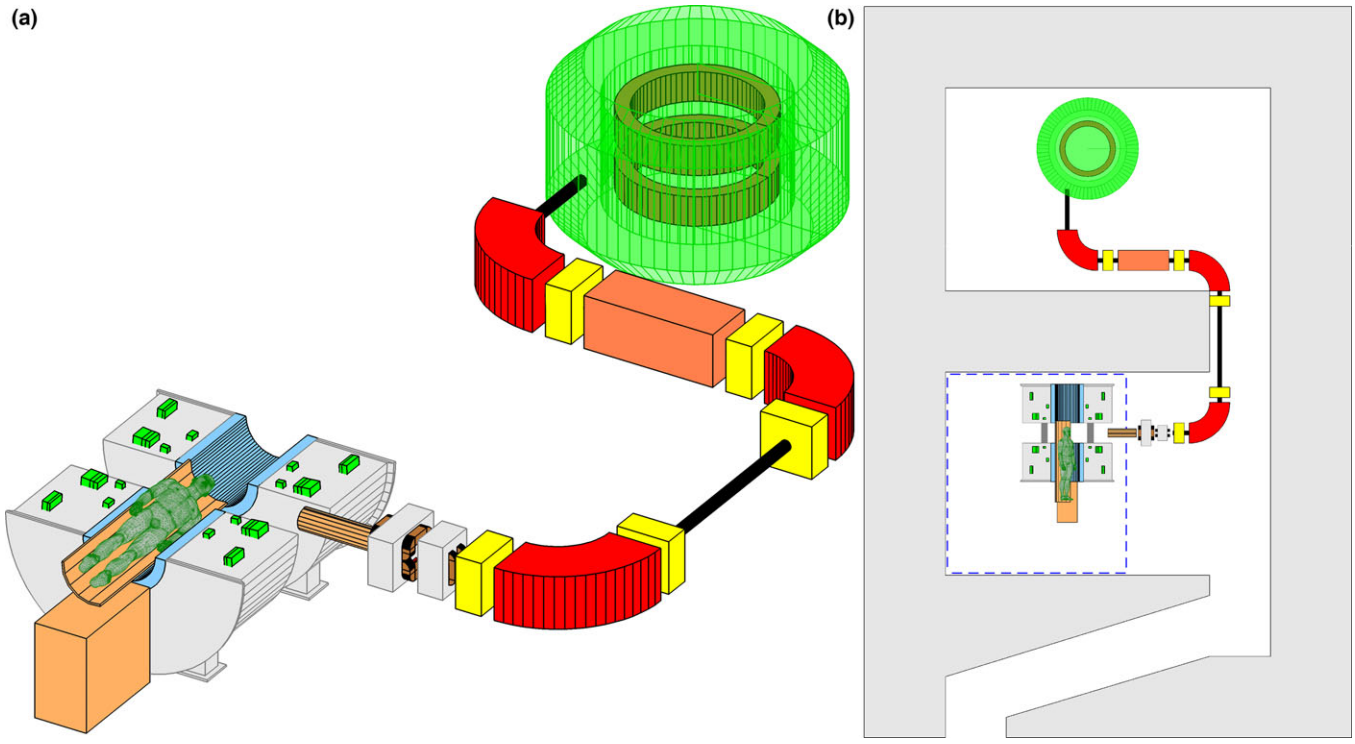

FIG. 3. MRPT prototype in the perpendicular orientation with an axially rotating couch design (no gantry). (a) shows a 3D cutaway view while (b) shows a top-view of the full bunker layout. An RF shield boundary is shown decoupling the MRI from the proton beamline (dashed line). The remaining proton beamline components are indicated by generic volumes such as scanning magnets, focusing quadrupoles, vacuum tubes, dipole magnets, energy selection system, and synchrocyclotron. The overall size of the bunker floor plan is $12 \times 18\,m^2$. [Color figure can be viewed at wileyonlinelibrary.com]

and inline) for systems where either the patient axially rotates (Figs. 3 and 5), or there is a gantry present (Figs. 4 and 6), in order for multiple beam angles to be delivered. In each figure, the basics of a surrounding radiation bunker are shown and the footprint described detailing the full proton beamline from accelerator to nozzle. A unique requirement of the systems with rotating gantry is that the mass of the MRI scanner must be considered — in the current 1 T system, this is around 12,000 kg.

5.A. Perpendicular orientation system

5.A.1. Rotating couch design

Figure 3 displays a perpendicular orientation MRPT system with an axially rotating couch (nongantry). Part (a) displays a 3D image showing a cutaway view of the MRI scanner and proton beamline. In this orientation, the PBS assembly directs a pencil beam through the magnet split-bore gap. The gross deflection of the pencil beam via the fringe field will be either up or down (depending on the MRI source coil current direction). In Fig. 3(b), a topview is shown which details the full layout of the radiation treatment bunker. The RF boundary is also indicated to isolate the MRI from the proton beamline. Of concrete shielding, 2 m is present on all walls and the MRI is shielded from the accelerator room and energy selection system. Additional magnetic shielding of the MRI fringe field beyond the bunker may be required depending on the location. The overall size of the bunker floor plan is $12 \times 8\ m^2$

5.A.2. Rotating gantry design

Figure 4 shows the perpendicular MRPT design with gantry (static couch). The design shown has the primary feature of a centrally mounted concrete pillar which houses the 12,000 kg MRI. By nature, this column prevents complete gantry 360° rotation and so a range of 300° (−150° to +150°) is estimated with the missing 60° zone being through the patient couch. The beamline would be mounted within a large barrel-style gantry that would be supported by rollers at the base. The RF shield would also need to wrap around the MRI scanner. In terms of bunker size, the rotating gantry only adds a few meters in the width direction to the nongantry design. The total footprint of the proposed layout is $14 \times 18\ m^2$.

5.B. Inline orientation system

5.B.1. Rotating couch design

Figure 5 displays the inline orientation system with an axially rotating couch (nongantry). In this case, the PBS assembly directs a pencil beam straight down the MRI bore. The

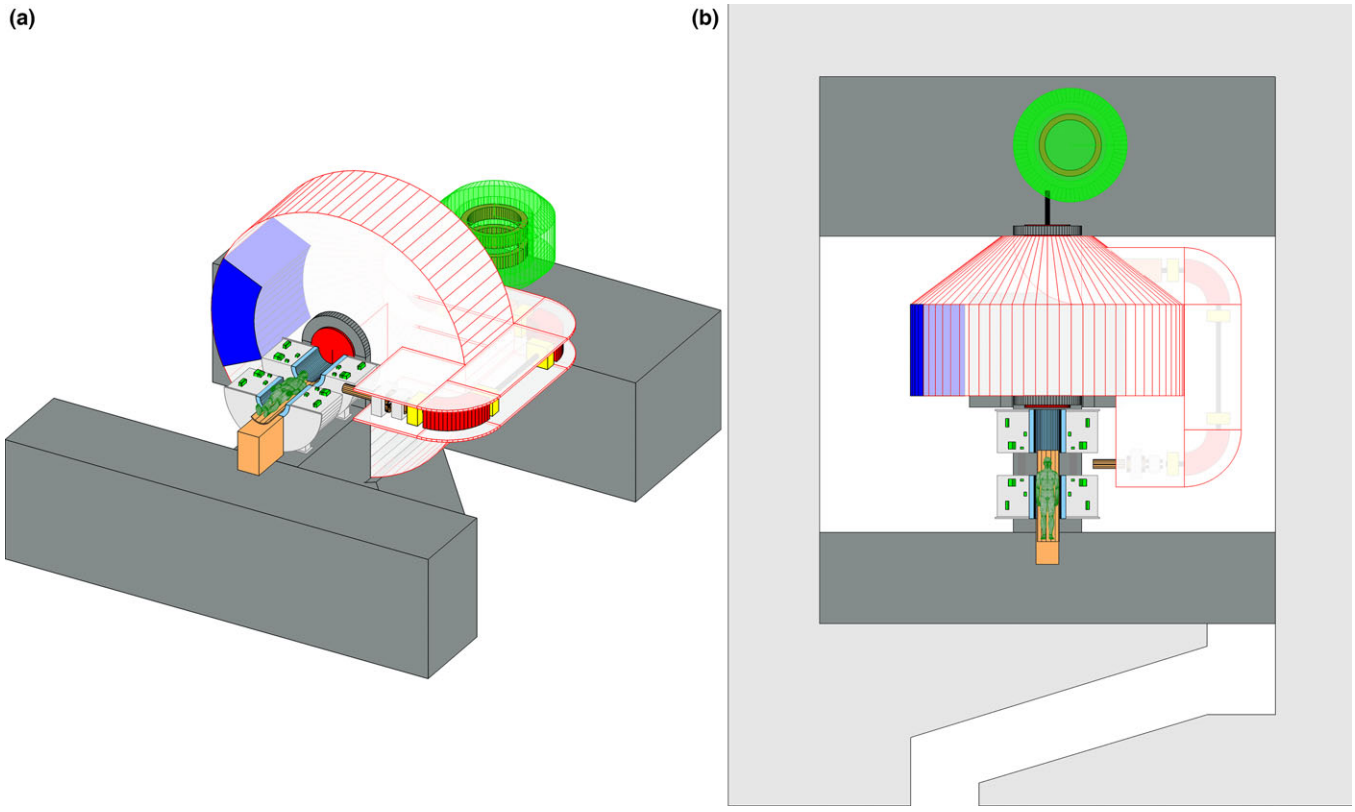

FIG. 4. Diagram of the MRI-guided proton therapy bunker layout in the perpendicular orientation. (a) 3D cutaway view (b) Topview detailing the entire bunker floor plan. The total footprint of the proposed layout is $14 \times 18\ m^2$. [Color figure can be viewed at wileyonlinelibrary.com]

gross deflection of the pencil beam via the fringe field will be rotation around the beam central axis either clockwise or anticlockwise (depending on the MRI source coil current direction).

5.B.2. Rotating gantry design

Figure 6 shows an example case of the rotating gantry design with inline magnetic field. In this case, the entire MRI system needs rotating, a unique engineering concept that appears feasible; we note the 0.5 T field MRI system in the Aurora RT design has a unique rotating biplanar MRI. For support of a 12,000 kg MRI and proton beam gantry, a large barrel-style gantry is envisaged as shown. The overall bunker size is identical to the perpendicular rotating gantry model at $14 \times 18\,m^2$

6. TOWARDS MRPT

Based on the ground-breaking advances seen through the development of MRXT, it could be expected that the development of MRPT will follow soon. In Sections 3 and 4, we have covered the various software and hardware elements that we predict to be important in the eventual realization of MRPT. In this section, we list our predictions for some of these key milestones. These developments will likely take a path that is determined by the utilization of existing technology coupled with gradual integration of the many components required.

6.A. Scanning magnet operation in MRI fringe fields

This exercise may be performed over several stages, and need not involve a complete proton therapy beamline. For example, a standalone pencil beam scanning unit may be tested in the vicinity of an MRI scanner. This would involve operating the scanning magnets at coil currents covering the full range of clinical treatment scenarios while recording MR images on a distortion phantom. The fringe field of the scanning magnet assembly may interfere with the MRI and vice versa. Image quality can be assessed directly by examining the distortion phantom image quality, while the scanning ability can be deduced from magnetic field measurements taken inside the scan magnet deflection volumes. If successful, then no significant changes would be expected once incorporated into a full static proton beamline with particles.

6.B. MRI-only proton therapy planning

Successful MRI-only planning will be self-evident starting from phantom studies. For example, anatomically accurate phantoms with various tissue analog inserts can be imaged in both CT and MRI systems with identical setups. From there identical plans can be made and experimental testing performed with dosimeters such as film present to verify the dosimetry differences between the two approaches. The dose calculation component of this dose planning process can also be performed in the Monte Carlo environment to compare predictions. Using these approaches, it can be expected that

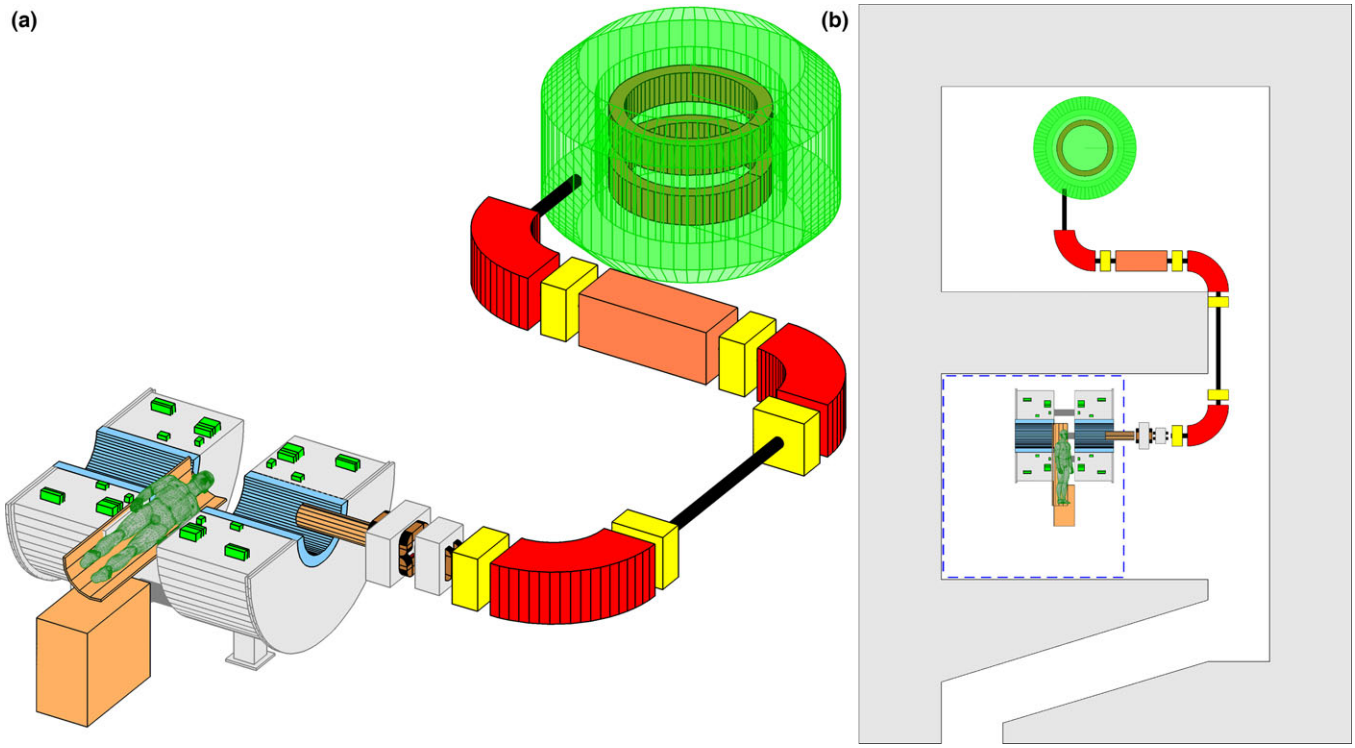

FIG. 5. MRPT prototype in the inline orientation with an axially rotating couch design (no gantry). (a) shows a 3D cutaway view while (b) shows a topview of the bunker layout. The overall size of the bunker floor plan is $12 \times 18\,m^2$. [Color figure can be viewed at wileyonlinelibrary.com]

incremental improvements will be achieved at regular intervals in progressing the accuracy of MRI-only data for dose planning.

6.C. Pencil beam scanning monitoring

Static beamline systems fitted with a pencil beam scanning system may be sufficient to examine this area of research in the early stages. It could be possible to emulate the fringe field of an MRI with a portable Helmholtz coil or similar system. Pencil beam monitors could be placed inside and measurements performed of the changes introduced by the magnetic field. Experimental work coupled with Monte Carlo modeling would be expected to accelerate any further development required to make such systems operate successfully in magnetic fields.

6.D. MRI compatible gantry development

Beyond the early stage static beamline prototype systems, research into complete integrated gantry designs may naturally follow. Introduction of existing gantry components, such as dipole bending magnets and gantry structures, into the fringe field of a nonclinical MRI system may be a realistic first approach. In parallel with this, modeling should be an attractive alternate method to predict the performance of a fully integrated system. Confidence would be gained from the preliminary experiments before construction of larger prototype designs.

6.E. Clinical trials

Similar to MRXT, clinical trials would form an important element in the implementation of MRPT. Current CT-planning-based proton therapy is indicated as being superior to CT-planning for photons for around 20% of cancer sites.[58] A fundamental argument in the desire to create MRPT is that the modality will be improved. This naturally would convert to greater superiority of proton beams over photons for even more cancer sites. Clinical trials will be the purest measure of the success of MRPT. As shown in Fig. 1, we envisage that common intrafractional static cancer sites such as brain to be investigated initially. Slightly more mobile sites such as prostate and head and neck would be next to be investigated. Finally, the more challenging dynamic intrafractional motion tumor sites would be examined such as lung, liver and abdomen.

7. DISCUSSION AND CONCLUSIONS

Protons were first regarded as a potential particle for use in radiotherapy by Robert Wilson in 1946.[59] The first

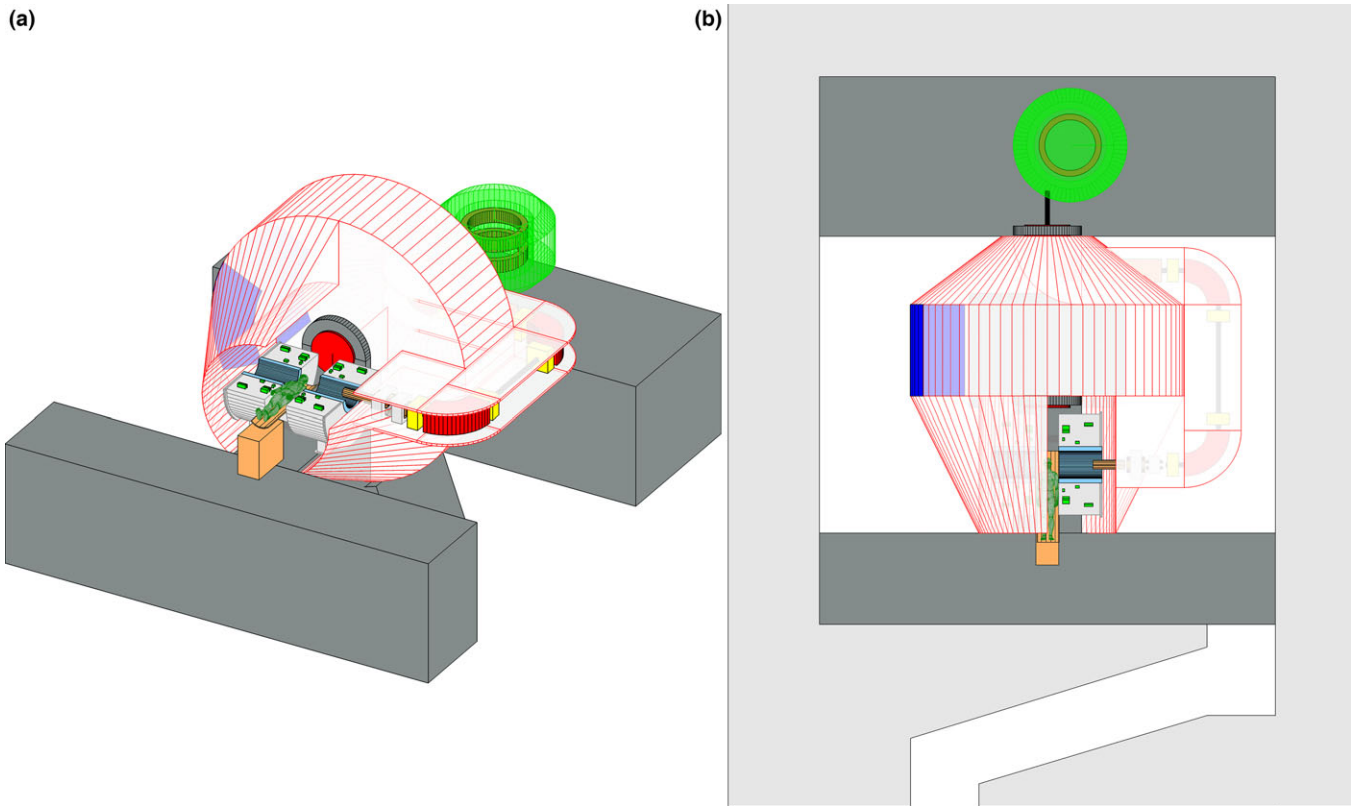

FIG. 6. Diagram of the MRI-guided proton therapy bunker layout in the inline orientation. (a) 3D cutaway view. (b) Topview detailing the bunker layout. In the design shown the gantry would be able to rotate from approximately −150 to +150 deg. The total footprint of the proposed layout is $14 \times 18\,m^2$. [Color figure can be viewed at wileyonlinelibrary.com]

reported treatments followed in 1955 at Lawrence Berkeley Laboratory,[60] and then after much delay, a hospital-based treatment program commenced at the Loma Linda University Medical Centre in 1990. Between 1990 and 2008, proton therapy continually spread and became recognized as a superior particle for radiotherapy treatments such as skull-based tumors and pediatric cases where a low integral dose is important due to the finite range of protons. In 2009, Smith published a Vision 20/20 article entitled "Proton Therapy".[61] In this paper, the overwhelming predictions for the coming decade were that intensity-modulated proton beam therapy would be a key element in bringing proton therapy forward. Along with this, several new centers were anticipated, and the cost of proton therapy was expected to decrease dramatically with advances in accelerator technology and single room gantry solutions becoming available. Based on analysis of data from the PTCOG website,[62] in 2009 about 52 proton beamlines were in operation worldwide. As of December 2016, about 162 are now in operation. It would appear that these predictions of the rapid expansion of proton therapy to be in good agreement with, if not exceed, the predictions of Smith from 2009. However rather interestingly, there was very little discussion on image guidance in the article. In fact, proton-CT was discussed as a potential technology that could improve treatment verification or planning accuracy. There was a very brief mention of anticipated cone-beam CT development, but no mention of MRI. In the 7 yr, from 2009 to 2016, we have witnessed a rapid progression of image-guided radiotherapy for x-ray beam therapy. The bar has been raised for expectations on how we guide a patients' radiation beam, and how we use images for dose planning. As described in detail throughout the current article, the latest milestone in x-ray beam radiotherapy is that of real-time MRI guidance. It has arguably been these developments that have pressured a dramatic shift in the proton therapy community. Cone-beam CT[63] and even in room CT systems are now in operation in several proton therapy centers.[64] We therefore predict that real-time MRI-guided proton beam therapy, MRPT, is potentially the next major advance in current proton beam radiotherapy practice. It will in principle offer enhancements that are unique to proton beam therapy, and should benefit the modality more than what MRI guidance offers x-ray therapy. The steps required to realize this new technology will be both software- and hardware-based. Software processes will need to be developed for robust planning and guidance with real-time MR images specific to proton beam therapy. Significant engineering work on new gantry designs will need to be performed. Further to this, it is expected that work will be required to ensure that beam delivery verification methods are accurate and support the concept of a more targeted radiotherapy. MRPT promises to expand on and further improve the current best quality treatment offered for various cancer sites by pure proton therapy. This will strengthen the visions from 1946 by Robert Wilson regarding the use of proton beams for cancer therapy, albeit some 80 yr down the track.

ACKNOWLEDGMENTS

The authors acknowledge funding from NHMRC Program Grant No. 1036078, ARC Discovery Grant No. DP120100821, and from a Research Grant with Ion Beam Applications (IBA), Belgium.

CONFLICTS OF INTEREST

The authors have no relevant conflicts of interest to disclose.

[a)]Author to whom correspondence should be addressed. Electronic mail: brad.oborn@gmail.com.

REFERENCES

1. Bentzen SM, Constine LS, Deasy JO, et al. Quantitative analyses of normal tissue effects in the clinic (quantec): an introduction to the scientific issues. *Int J Radiat Oncol Biol Phys*. 2010;76:S3–S9.
2. Yu JB, Soulos PR Herrin J, et al. Proton versus intensity-modulated radiotherapy for prostate cancer: patterns of care and early toxicity. *J Natl Cancer Inst*. 2013;105:25–32.
3. Komaki R, Gomez DR, O'Reilly M, et al. Bayesian randomized trial comparing intensity modulated radiation therapy versus passively scattered proton therapy for locally advanced non-small cell lung cancer. *J Clin Oncol*. 2016;34:25–32.
4. Paganetti H, Yu CX, Orton CG. Photon radiotherapy has reached its limit in terms of catching up dosimetrically with proton therapy. *Med Phys*. 2016;43:4470–4472.
5. Mutic S. Dempsey JF. The ViewRay system: magnetic resonance – guided and controlled radiotherapy. *Semin Radiat Oncol*. 2014;24:196–199.
6. ViewRay. Mridian treatment centres. 2016. http://www.viewray.com/treatment-centers, Accessed December 1 2016.
7. ViewRay. Newsroom. 2016. http://www.viewray.com/newsroom, Accessed December 1 2016.
8. ViewRay. Viewray treatments are visibly different. 2016. http://www.viewray.com/product, Accessed December 1 2016.
9. ViewRay. Washington university acquires Viewray research system to investigate MRI-guided linac capabilities. 2016. http://www.viewray.com/press-releases/washington-university-acquires-viewray-research-system-to-investigate-mri-guided-linac-capabilities, Accessed Feb 21 2017.
10. Lagendijk JJW, Raaymakers BW, van Vulpen M. The magnetic resonance imaging-linac system. *Semin Radiat Oncol*. 2014;24:207–209.
11. Elekta. Elekta landing page. 2016. https://static.elekta.com/mr-linac/, Accessed December 1 2016.
12. Magnettx. The future of radiotherapy is MRI guided. 2016. http://www.-magnettx.com/, Accessed December 1 2016.
13. Fallone BG. The rotating biplanar linac – magnetic resonance imaging system. *Semin Radiat Oncol*. 2014;24:200–202.
14. University of Alberta. Linac-MR project links. 2016. http://www.mp.med.ualberta.ca/linac-mr/publications.html, Accessed December 1 2016.
15. Keall PJ, Barton M. Crozier S. The Australian magnetic resonance imaging – linac program. *Semin Radiat Oncol*. 2014;24:203–206.
16. Liney GP, Dong B, Begg J, et al. Technical note: experimental results from a prototype high-field inline MRI-linac. *Med Phys*. 2016;43:5188–5194.
17. University of Sydney. MR-linac program. 2016. http://sydney.edu.au/medicine/radiation-physics/research-projects/MRI-linac-program.php, Accessed December 1 2016.
18. Raaymakers BW, Raaijmakers AJE, Lagendijk JJW. Feasibility of MRI guided proton therapy: magnetic field dose effects. *Phys Med Biol*. 2008;53:5615–5622.

19. Wolf R, Bortfeld T. An analytical solution to proton Bragg peak deflection in a magnetic field. *Phys Med Biol*. 2012;57:N329–N337.
20. Moteabbed M, Schuemann J, Paganetti H. Dosimetric feasibility of real-time MRI-guided proton therapy. *Med Phys*. 2014;41:111713 (11pp).
21. Hartman J, Kontaxis C, Bol GH, et al. Dosimetric feasibility of intensity modulated proton therapy in a transverse magnetic field of 1.5 T. *Phys Med Biol*. 2015;60:5955.
22. Oborn BM, Dowdell S, Metcalfe PE, Crozier S, Mohan R, Keall PJ. Proton beam deflection in MRI fields: implications for MRI-guided proton therapy. *Med Phys*. 2015;42:2113–2124.
23. Rank CM, Hunemohr N, Nagel AM, Rothke MC, Jakel O, Greilich S. MRI-based simulation of treatment plans for ion radiotherapy in the brain region. *Radiother Oncol*. 2013;109:414–418.
24. Tremmel C, Hunemohr N, Nagel AM, Jakel O, Greilich S, Rank CM. MRI-based treatment plan simulation and adaptation for ion radiotherapy using a classification-based approach. *Radiat Oncol*. 2013;8:51.
25. Edmund JM, Kjer HM, Van Leemput K, Hansen RH, Andersen JAL, Andreasen D. A voxel-based investigation for MRI-only radiotherapy of the brain using ultra short echo times. *Phys Med Biol*. 2014;59:7501.
26. Koivula L, Wee L, Korhonen J. Feasibility of MRI-only treatment planning for proton therapy in brain and prostate cancers: dose calculation accuracy in substitute CT images. *Med Phys*. 2016;43:4634–4642.
27. Schippers JM, Lomax AJ. Emerging technologies in proton therapy. *Acta Oncol*. 2011;50:838–850.
28. ViewRay. Nonstop imaging supports advanced therapy tecnhiques. 2016. http://www.viewray.com/treatment, Accessed December 1 2016.
29. Colvill E, Poulsen PR, Booth JT, OBrien RT, Ng JA, Keall PJ. DMLC tracking and gating can improve dose coverage for prostate VMAT. *Med Phys*. 2014;41:091705.
30. Acharya S, Fischer-Valuck BW, Kashani R, et al. Online magnetic resonance image guided adaptive radiation therapy: first clinical applications. *Int J Radiat Oncol Biol Phys*. 2016;94:394–403.
31. Li Y, Kardar L, Li X, et al. On the interplay effects with proton scanning beams in stage III lung cancer. *Med Phys*. 2014;41:021721.
32. Dowdell S, Grassberger C, Sharp GC, Paganetti H. Interplay effects in proton scanning for lung: a 4D Monte Carlo study assessing the impact of tumor and beam delivery parameters. *Phys Med Biol*. 2013;58:4137.
33. Grassberger C, Dowdell S, Sharp G, Paganetti H. Motion mitigation for lung cancer patients treated with active scanning proton therapy. *Med Phys*. 2015;42:2462–2469.
34. Zhang Y, Knopf A, Tanner C, Lomax AJ. Online image guided tumour tracking with scanned proton beams: a comprehensive simulation study. *Phys Med Biol*. 2014;59:7793.
35. Han D, Siebers JV, Williamson JF. A linear, separable two-parameter model for dual energy CT imaging of proton stopping power computation. *Med Phys*. 2016;43:600–612.
36. Zhu J, Penfold SN. Dosimetric comparison of stopping power calibration with dual-energy CT and single-energy CT in proton therapy treatment planning. *Med Phys*. 2016;43:2845–2854.
37. Taasti VT, Petersen JBB, Muren LP, Thygesen J, Hansen DC. A robust empirical parametrization of proton stopping power using dual energy CT. *Med Phys*. 2016;43:5547–5560.
38. Dowling JA, Lambert J, Parker J, et al. An atlas-based electron density mapping method for magnetic resonance imaging (MRI)-alone treatment planning and adaptive MRI-based prostate radiation therapy. *Int J Radiat Oncol Biol Phys*. 2012;83:e5–e11.
39. Dowling JA, Sun J, Pichler P, et al. Automatic substitute computed tomography generation and contouring for magnetic resonance imaging (MRI)-alone external beam radiation therapy from standard MRI sequences. *Int J Radiat Oncol Biol Phys*. 2015;93:1144–1153.
40. Arabi H, Koutsouvelis N, Rouzaud M, Miralbell R, Zaidi H. Atlas-guided generation of pseudo-CT images for MRI-only and hybrid PETMRI-guided radiotherapy treatment planning. *Phys Med Biol*. 2016;61:6531.
41. Oborn BM, Metcalfe PE, Butson MJ, Rosenfeld AB. High resolution entry and exit Monte Carlo dose calculations from a linear accelerator 6 MV beam under influence of transverse magnetic fields. *Med Phys*. 2009;36:3549–3559.
42. Oborn BM, Metcalfe PE, Butson MJ, Rosenfeld AB. Monte Carlo characterization of skin doses in 6 MV transverse field MRI-linac systems: effect of field size, surface orientation, magnetic field strength, and exit bolus. *Med Phys*. 2010;37:5208–5217.
43. Oborn BM, Metcalfe PE, Butson MJ, Rosenfeld AB, Keall PJ. Electron contamination modeling and skin dose in 6 MV longitudinal field MRIgRT: impact of the MRI and MRI fringe field. *Med Phys*. 2012;39:874–890.
44. Oborn BM, Kolling S, Metcalfe PE, Crozier S, Litzenberg DW, Keall PJ. Electron contamination modeling and reduction in a 1 T open bore inline MRI-linac system. *Med Phys*. 2014;41:051708 (15pp).
45. van Heijst TCF, den Hartogh MD, Lagendijk JJW, van den Bongard HJGD, van Asselen B. MR-guided breast radiotherapy: feasibility and magnetic-field impact on skin dose. *Phys Med Biol*. 2013;58:5917–5930.
46. Keyvanloo A, Burke B, Warkentin B, et al. Skin dose in longitudinal and transverse linac-MRIs using Monte Carlo and realistic 3D MRI models. *Med Phys*. 2012;39:6509–6521.
47. Keyvanloo A, Burke B, Aubin JS, et al. Minimal skin dose increase in longitudinal rotating biplanar linac-MR systems: examination of radiation energy and flattening filter design. *Phys Med Biol*. 2016;61:3527.
48. Raaijmakers AJE, Raaymakers BW, Lagendijk JJW. Integrating a MRI scanner with a 6 MV radiotherapy accelerator: dose increase at tissue-air interfaces in a lateral magnetic field due to returning electrons. *Phys Med Biol*. 2005;50:1363–1376.
49. Raaijmakers AJE, Raaymakers BW, van der Meer S, Lagendijk JJW. Integrating a MRI scanner with a 6 MV radiotherapy accelerator: impact of the surface orientation on the entrance and exit dose due to the transverse magnetic field. *Phys Med Biol*. 2007;52:929–939.
50. Raaijmakers AJE, Raaymakers BW, Lagendijk JJW. Magnetic-field-induced dose effects in MR-guided radiotherapy systems: dependence on the magnetic field strength. *Phys Med Biol*. 2008;53:909–923.
51. Giantsoudi D, Schuemann J, Jia X, Dowdell S, Jiang S, Paganetti H. Validation of a GPU-based Monte Carlo code (pPMC) for proton radiation therapy: clinical cases study. *Phys Med Biol*. 2015;60:2257.
52. Wan Chan Tseung H, Ma J, Beltran C. A fast GPU-based Monte Carlo simulation of proton transport with detailed modeling of nonelastic interactions. *Med Phys*. 2015;42:2967–2978.
53. Chaudhri N, Saito N, Bert C, et al. Ion-optical studies for a range adaptation method in ion beam therapy using a static wedge degrader combined with magnetic beam deflection. *Phys Med Biol*. 2010;55:3499.
54. Paganetti H. Relative biological effectiveness (RBE) values for proton beam therapy variations as a function of biological endpoint, dose, and linear energy transfer. *Phys Med Biol*. 2014;59:R419.
55. Dewhirst MW, Birer SR. Oxygen-enhanced MRI is a major advance in tumor hypoxia imaging. *Can Res*. 2016;76:769–772.
56. O'Connor JPB, Boult JKR, Jamin Y, et al. Oxygen-enhanced MRI accurately identifies, quantifies, and maps tumor hypoxia in preclinical cancer models. *Can Res*. 2016;76:787–795.
57. Yan S, Lu HM, Flanz J, Adams J, Trofimov A, Bortfeld T. Reassessment of the necessity of the proton gantry: analysis of beam orientations from 4332 treatments at the Massachusetts General Hospital proton center over the past 10 years. *Int J Radiat Oncol Biol Phys*. 2016;95:224–233.
58. Health Council of the Netherlands. Horizon scanning report on proton radiotherapy. 2008. http://www.gezondheidsraad.nl/en/task-and-procedure/areas-of-activity/optimum-healthcare/proton-radiotherapy, Accessed December 1 2016.
59. Wilson RR. Radiological use of fast protons. *Radiology*. 1946;47:487–491.
60. Tobias CA, Lawrence JH, Born JL, et al. Pituitary irradiation with high-energy proton beams a preliminary report. *Can Res*. 1958;18:121–134.
61. Smith AR. Vision 2020: proton therapy. *Med Phys*. 2009;36:556–568.
62. PTCOG. Facilities in operation. 2016. http://www.ptcog.ch/index.php/facilities-in-operation, Accessed December 1 2016.
63. MedicalPhysicsWeb. World's first proton therapy specific cone-beam CT goes clinical. 2016. http://medicalphysicsweb.org/cws/article/newsfeed/58614, Accessed December 1 2016.
64. MedicalPhysicsWeb. IBA installs its first in-room CT-on-rails at Trento proton therapy center. 2016. http://medicalphysicsweb.org/cws/article/newsfeed/60462, Accessed December 1 2016.